Identification of Key Sequence Determinants for the Inhibitory Function of the Prodomain of TACE[†]

Patricia E. Gonzales,[‡] Jennifer D. Galli,[§] and Marcos E. Milla*[,||]

Department of Biochemistry and Biophysics, University of Pennsylvania School of Medicine, Philadelphia, Pennsylvania 19104

Received June 3, 2008; Revised Manuscript Received July 15, 2008

ABSTRACT: The TNFα converting enzyme (TACE) is a zinc metalloproteinase that mediates shedding of multiple cell surface proteins. Regulation of TACE enzymatic activity is ultimately mediated via proteolytic removal of its inhibitory prodomain. Sequence determinants for TACE prodomain inhibition of the catalytic domain are yet to be identified. Surprisingly, although TACE and ADAM 10 (closest homologue) share only 23% sequence identity at their prodomains, the latter in isolation inhibits TACE with the same potency as TACE own prodomain. In contrast, the prodomain of ADAM 9 inhibited TACE only weakly. Detailed analysis of ADAM prodomains revealed two short regions for which TACE and ADAM 10 depart dramatically from all other family members. We prepared TACE prodomain variants containing full or partial switches to ADAM 9 residues at those two regions and examined their functional properties. Variants containing ADAM 9 substitutions including amino acid residues 72−82 and 126−137 were fully inactive for TACE inhibition. A third variant comprising residues 114−125 was active but at lower potency relative to wild type. All inactive variants appeared to be correctly folded. Finally, the amino acid residue Phe72 and the motif Asp-Asp-Val-Ile137 were identified within those regions as key determinants for TACE prodomain inhibitory function. We conclude that TACE and ADAM 10 prodomains are functionally equivalent in a way that separates them from the rest of the ADAM family.

TACE[1] is an essential proteolytic activity mediating the conversion of proTNFα to its secreted form, and its physiological role has been demonstrated *in vitro* and *in vivo* (*1, 2*). TACE is also critical for the secretion of a large number of cell surface proteins such as transforming growth factor-α (*3*−*6*), TNF receptors I and II (*7*), the heparin-binding endothelial growth factor (*8*), the erbB4/HER4 epidermal growth factor receptor isoform JM-a (*9*), the growth hormone receptor (*10*), the macrophage colony-stimulating factor receptor (*11*), Notch-1 (*12*), the amyloid precursor protein (*13*−*15*), the cellular prion protein PrP^C (*16*), among others. Many of these ectodomains have critical roles in carcinogenesis, inflammation, and other pathologies.

Despite intense research into the biogenesis and substrate specificity of TACE and other ADAM family members, surprisingly little is known about how these enzymes are activated, the role of their prodomains in the control this process, and how substrate recognition takes place and is regulated. Our group and others have found that the TACE prodomain is essential for secretion of this enzyme in a functional form. We have shown that TACE expression constructs that lack the prodomain in its entirety failed to drive the secretion of functional enzyme in insect cells. The protein that is made is retained in the endoplasmic reticulum and subject to degradation (*17*). Therefore, the prodomain of TACE appears to work as an intramolecular chaperone, aiding in the secretion of this proteinase. The complementarity between the prodomain and the catalytic domain is indicated by both their tight mutual association and the fact that the prodomain is also degraded when expressed separate from the catalytic domain. Similar results were obtained with full-length TACE constructs (*18*).

ADAM prodomains also mediate inhibition of immature forms of these enzymes. Several ADAMs have been the subject of studies focusing on the prodomain-mediated dual role in enzyme secretion and inhibition: ADAM 8 (*19, 20*), ADAM 9 (*21*), ADAM 10 (*20, 22*), ADAM 12 (*23, 24*), ADAM 15 (*25*), ADAM 17 (TACE *17, 26, 27*), ADAM 19 (*28*), and ADAM 28 (*29*). All of these family members require the presence of the prodomain for secretion. In each case, it has been shown in cell-based assays or with partially purified ADAM preparations that the zymogen is inactive. ADAM prodomains are similar to matrix metalloproteinases in that they possess a short consensus sequence toward their C-terminus including a cysteine residue. This motif, named the "cysteine switch" is involved in coordination of the zinc ion at the active site of the catalytic domain of matrix metalloproteinases and is critical for zymogen inhibition (*30, 31*). The studies that addressed cysteine switch function in ADAMs yielded differing observations. For ADAM 12, the

[†] This research was supported by Grant AR-45949 from the National Institute for Arthritis and Musculoskeletal Diseases, NIH.

* Corresponding author. Phone: 650-855-5622. Fax: 650-852-1700. E-mail: marcos.milla@roche.com.

[‡] Present address: Department of Chemistry, Pontificia Universidad Catolica del Peru, Lima, Peru.

[§] Present address: Merck Research Laboratories, West Point, PA 19486.

[||] Present address: Roche Pharmaceuticals, 3431 Hillview Ave., Mailstop R2-101, Palo Alto, CA 94304.

[1] Abbreviations: TNFα, tumor necrosis factor-α; TACE, TNFα converting enzyme; ADAM, a disintegrin and metalloproteinase; IPTG, isopropyl β-D-thiogalactoside; Gdn-HCl, guanidine hydrochloride; SDS, sodium dodecyl sulfate; Dnp, dinitrophenyl.

10.1021/bi801049v CCC: $40.75
Published on Web 08/16/2008

```
TACE     ---MRQSLLFLTSVVPFVLAPRPPDDPGFGPHQRLEKLDSLLSDYDILSLSNIQQHSVRKRDLQTSTHVETLLTFSAL 75
ADAM 10  --------MVLLRVLILLLSWAAGMGGQYGNPLNKYIRHYEGLSYNVDSLHQKHQRAKRAVSHEDQF---LRLDFHAH 67
ADAM 9   --MGSGARFPSGTLRVRWLLLLGLVGPVLGAARPGFQQTSHLSSYEIITPWRLT-RERREAPRPYSKQVSYVIQAEGK 75

TACE     KRHFKLYLTSSTERFSQNFKVVVVDGKNESEYTVKWQDFFTGHVVGEPDSRVLAHIRDDDVIIRINTDGAEYNIEPLW 153
ADAM 10  GRHFNLRMKRDTSLFSDEFKVETSN-KVL-DYDTSH--IYTGHIYGEEGSFSHGSVIDGRFEGFIQTRGGTFYVE--- 138
ADAM 9   EHIIHLERNKD-LLPED-FVVYTYN-KEGTLITDHPN-IQNHCHYRGYVEGVHNSSIALSDCFGLRGLLHLENAS--- 146

TACE     R-----FVNDTKDKRMLVYKSEDIKNVSRLQSPKVCGYLKVDNEELLPKGLVDREPPEELVH----------RVKRR 215
ADAM 10  PAER-YIKDRTLPFHSVIYHEDDINYPHKYGPQGGCADHSVF--ERMRKYQMTGV--EEVTQIPQEEHAANGPELLRK 211
ADAM 9   ---YGIEPLQNSSHFEHIIYRMDDVYKE----PLKCGVSNKDI-EKETAKDEEEEPP-SMTQ----------LLRR 203
```

FIGURE 1: Sequence alignment of the prodomains of TACE (ADAM 17), ADAM 9, and ADAM 10. Bold letters: identical amino acid residues. Gray box: cysteine switch motif. Arrow: furin maturation site.

switch is essential for inhibitory activity (*23*), while for TACE and ADAM 10, it is not necessary (*20, 27*). This may set TACE and ADAM 10 apart from all other ADAM family members and most metzincins.

For TACE, removal of its inhibitory prodomain is mediated by members of the furin/KEX-2 family of proprotein converting enzymes of the trans-golgi network (*32, 33*). Our evidence indicates that the potency of the prodomain as a TACE inhibitor dramatically depends on the presence of the cysteine-rich/disintegrin domain, localized between the C-terminus of the catalytic domain and the start of the yuxtamembrane region: the prodomain is much less capable of inhibiting this form relative to the catalytic domain in isolation (*27*). We confirmed this conclusion by showing that the isolated disintegrin/cysteine-rich domain can effect the dissociation of inhibited prodomain−catalytic domain complexes. Therefore, proteolytic activation constitutes a regulatory step, involving at least a topological component given by the availability of precursor TACE and the processing protease (proprotein convertase) within the same subcellular compartment.

The chaperone function of TACE prodomain is not mediated by its cysteine switch motif (PKV**C**GYLK188), as initially thought by analogy to other prodomain-containing metzincins. Several groups have hypothesized that the cysteine residue of that motif serves a key role in the association of the prodomain with the catalytic domain and its inhibition, via ligation of the Zn^{2+} ion within the active site of the enzyme. We found that a C184A point mutant of TACE was secreted into culture media as efficiently as its wild-type counterpart, and the secreted enzyme was active (*18*). This result suggested that C184 is not essential for the biogenesis and maturation of the protease. Likewise, prodomain variants containing the C184A mutation alone or paired with single alanine substitutions along the cysteine switch inhibit the enzyme with equal potency as wild-type TACE prodomain. Other residues within the prodomain must determine its interaction with the catalytic domain as part of the assembly and trafficking of this protein through the secretory pathway and for inhibition for its proteolytic activity. In this paper, we report on the discovery of two discrete segments within the prodomain of TACE that contribute to its association with the catalytic domain and inhibition of this enzyme.

MATERIALS AND METHODS

Generation of ADAM 9 and ADAM 10 Pro Plasmids. A plasmid for expression of the prodomain of TACE lacking the signal peptide in *Escherichia coli*, using the vector pRSET B TACE Pro, was described before (*27*). A DNA fragment encoding residues Pro25 to Arg205 of ADAM9 with an *Sma*I site at the 5′-end and *Bam*HI site at the 3′-end was generated by polymerase chain reaction amplification using a previously reported pFastBac1 ADAM 9 plasmid as a template (*21, 34, 35*). The fragment was inserted at the *Bam*HI and *Sma*I sites of TACE Pro to obtain AD9 Pro. AD10 Pro was generated in a similar fashion with a fragment encoding residues Pro26 to Arg215 of ADAM 10 and using a preexisting pFastBac1 ADAM 10 plasmid as a template (*36*).

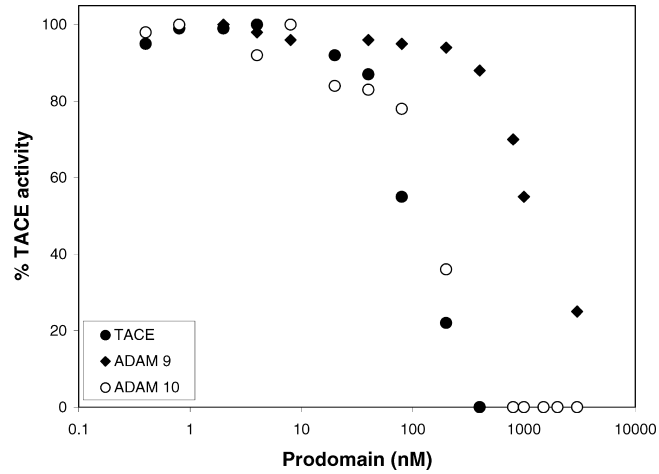

FIGURE 2: Inhibition of TACE catalytic domain (residues 215−473) by recombinant, purified prodomains from TACE, ADAM 10, and ADAM 9. Each curve is representative of at least three experiments.

Generation of Mutant Region Plasmids. We prepared TACE variants in which the residues of regions 1 and 2 were mutated to those of ADAM 9 (Figures 3 and 4). The following mutants were constructed by cassette mutagenesis using as backbone pBlueScript encoding human TACE cDNA with a stop codon at the end of the catalytic domain (TACE R473 *17, 18*): R473/1, R473/Reg1A, R473/1B, R473/2, R473/2A, and R473/2B. To facilitate cassette insertion, three unique restriction sites were engineered into the prodomain-encoding region of pBS/TACE-R473: *Sal*I at codon 99, *Nru*I at codon 125, and *Sph*I at codon 163. All of these base substitutions were silent. Oligonucleotide cassettes for R473/1, R473/1A, and R473/1B were synthesized with *Bgl*II and *Sal*I compatible ends for insertion into pBS/TACE-R473 previously cleaved with those enzymes. Owing to the size and location of region 2, variants R473/2A and R473/

REGION 1		
TACE	FSALKRHFKLYLTSSTERFSQNFKV-96	identical residues
ADAM10	FHAHGRHFNLRMKRDTSLFSDEFKV	12/25(vs TACE)
ADAM12	LQRESKELIINLERNEGLIASSFTE	2
ADAM13	VSSEGRKFILKVERNHLLFAPGYTE	5
ADAM15	LELDGDSHILELLQNRELVPGRPTL	3
ADAM8	LGATGHNFTLHLRKNRDLLGSGYTE	4
ADAM9	IQAEGKEHIIHLERNKDLLPEDFVV	4
ADAM16	IMIDSKDYIIHLVHNPMLVTTDFKV	4
ADAM20	LRFGGQRYIVHMRVNKLLFAAHLPV	2
ADAM14	VIRSNQLGRLKLVLERNNFIFLNQT	3
ADAM22	VDAFGTSFILDVVLNHDLLSSEYIE	4
ADAM3	IKIEGKPYTFLL-EKQSFLHPHFLV	3
ADAM5	ITIEGKPYFVHL-KKQSILSSASFI	2
REGION 2		
TACE	--FFTGHVVGEPDSRVLAHIRD-DDVI-137	6/27 (vs consensus)
ADAM10	--IYTGHIYGEEGSFSHGSVID-GRFE	5
ADAM12	HCYYHGHVRGYSDSAVSLSTCS-GLRG	17
ADAM13	HCYYHGQVENYDESSVALTTCS-GISG	14
ADAM15	NCCYQGRVRGYAGSWVSICTCS-GLRG	14
ADAM8	HCLYQGHVEGYPDSAASLSTCA-GLRG	17
ADAM9	HCHYRGYVEGVHNSSIALSDCF-GLRG	16
ADAM16	HCYYQGYVQGYPNSVVAMNTCS-GLRG	19
ADAM20	DWYYHGYVEGVPESLVALSTCSGGFLG	16
ADAM14	NCYYQGTVGGEESSFVALSSCN-GLRG	17
ADAM22	HCYYQGHIRGNPDSFVALSTCH-GLHG	18
ADAM3	HCFYQGYVADIPKSAVTLRTCS-GLRG	17
ADAM5	DCNYNGYVAGIPNSLVTLSVCS-GLRG	16
CONSENSUS	HCYYQGYVXGXPXSXVALSTCX-GLRG	

FIGURE 3: Sequence alignment of the prodomains of TACE and 12 other ADAMs: region 1 (TACE residues 72−96) and region 2 (TACE residues 114−137). Bold letters: identical amino acid residues.

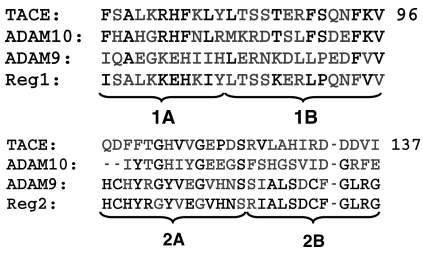

FIGURE 4: Design of TACE prodomain chimeras containing the ADAM 9 sequence of region 1 (panel A, top) or 2 (panel B, bottom). For TACE, ADAM 9, and ADAM 10, black letters indicate identical residues. For "region 1" and "region 2", gray letters indicate positions where the sequence remained the same as in TACE, while black letters indicate substitutions on the TACE prodomain sequence.

2B were constructed first and then assembled to produce 473/2. The 2A cassette was synthesized with *Sal*I and *Nru*I compatible ends for insertion into pBS/TACE-R473 treated with those enzymes. The 2B cassette was synthesized with *Nru*I and *Sph*I compatible ends for insertion on that same plasmid treated with *Nru*I and *Sph*I. Variant R473/2 was then constructed by inserting the 2B cassette into the R473/2A plasmid. Variants F72V and GLRG137 were constructed by replacement of the corresponding codons on the cassettes containing those positions.

All mutations were then transferred to a pRSET B vector by digesting both the corresponding donor pBS/TACE-R473 plasmid and the host pRSETB/TACE-Pro plasmid with *Sma*I and *Eco*RV. TACE ProReg2AD was generated by divergent PCR, using TACE ProReg2A as the template and primers carrying a Cys to Asp substitution in position 113. TACE ProReg2BR was also generated by divergent PCR using TACE ProReg2B as the template and primers carrying a Cys to Arg mutation in position 132.

Prodomain Expression in E. coli. BL21(DE3) electrocompetent cells were transformed with the corresponding pRSET B/TACE Pro plasmid and plated on LB agar containing 150 μg/mL ampicillin. After overnight incubation at 37 °C, cells were resuspended in 1 L of LB medium supplemented with 150 μg/mL ampicillin. Cells were grown at 37 °C up to an OD_{600} of 0.6 and then induced with 1 mM isopropyl β-D-thiogalactoside (IPTG). Harvesting by centrifugation was performed 3 h postinduction.

Purification and Refolding of TACE Pro and Variants. We essentially followed the protocol previously reported in ref *27*. Cell pellets were washed once with 20 mM Tris-HCl, pH 8, and twice with this same buffer containing 0.1% Triton X-100. Washed pellets were then solubilized in 20 mM Tris-HCl, pH 8, containing 6 M guanidine hydrochloride (Gdn-HCl) and centrifuged at 26000*g* for 30 min. The supernatant was applied to a 20 mL Ni-NTA column. The column was washed with 20 mM Tris-HCl, pH 8, and 6 M Gdn-HCl and then with this same buffer containing 20 mM imidazole. The protein was eluted with 20 mM Tris-HCl, pH 8, 6 M Gdn-HCl, and 300 mM imidazole. All proteins appeared to be over 95% homogeneous, as determined by Coomassie staining of SDS−polyacrylamide gels.

TACE prodomain refolding involved a series of steps including incubation with refolding buffer and dialysis (*27*). Briefly, purified protein eluates were dialyzed against water, causing formation of a white protein precipitate. That material was resuspended in 20 mM Tris-HCl, pH 8, and 6 M Gdn-HCl to a final concentration of 6 mg/mL. Aliquots of this protein solution were diluted at a 1:20 ratio with refolding buffer (FoldIt Screen formulation 16, Hampton Research: 55 mM Tris, pH 8.2, 264 mM NaCl, 11 mM KCl, 2.2 mM $MgCl_2$, 0.055% polyethylene glycol 3350, 550 mM Gdn-HCl, 440 mM sucrose, 550 mM L-arginine monohydrochloride), with addition of 1 mM reduced glutathione, 0.1 mM oxidized glutathione, and 3 mM lauryl maltoside. Dilutions were then incubated for 4 h at 4 °C with gentle stirring. Samples were then centrifuged at 10000*g* for 10 min and filtered using 0.22 μm PVDF membranes. Proteins were finally dialyzed against 20 mM Tris-HCl, pH 8, with 150 mM NaCl (buffer A). Under this condition, all prodomain variants were stable in solution for several days.

Expression and Purification of the Catalytic Domain of TACE and Inhibition Assays. The expression and purification of the catalytic domain of TACE as well as a functional assay have been described in ref *27*. In summary, the inhibitory activity of TACE prodomains was determined using the synthetic peptide Dnp-SPLAQAVRSSSR-NH_2 as substrate. This peptide comprises positions P_6 to $P_{6'}$ of the TACE cleavage site within the precursor TNF-α sequence. The catalytic domain of TACE at a final concentration of 1 nM was incubated with serial dilutions of prodomains in buffer A. Reactions were initiated by addition of substrate at a final concentration of 20 μM and then incubated at 37 °C for 30 min. They were then stopped by addition of 1 volume of 1% heptafluorobutyric acid. Quenched reaction mixtures were applied to a 150 mm C_{18} reverse-phase HPLC column (Vydac) and resolved using a multistep acetonitrile gradient in 0.1% heptafluorobutyric acid. TACE activity was measured by integration of the absorbance at 350 nm of substrate and product peaks and expressed as percent ratio using the formula % activity = $P_{350}/(P_{350} + S_{350})$, where P_{350} and S_{350} are the integrated absorbance at 350 nm of the product and substrate peaks, respectively.

Circular Dichroism (CD) Spectroscopy. CD spectra were recorded using an AVIV 62DS spectropolarimeter. Prodomain stocks were prepared at a concentration of 180 μM in buffer A containing 6 M Gdn-HCl. Those stocks were rapidly diluted 60-fold in buffer A to reach a final concentration of 3 μM. Spectra were collected in triplicate over the far-UV region (208−260 nm) using a 1 cm path fused quartz cuvette (Hellma).

RESULTS

The TACE and ADAM 10 Prodomains Are Functionally Equivalent as TACE Inhibitors. We have previously shown that the TACE prodomain can be expressed in isolation as a stably folded polypeptide (*27*). This domain associates with the catalytic domain and inhibits its proteolytic activity with or without a functional cysteine switch motif. Its potency does depend on whether or not the disintegrin/cysteine-rich domain is part of the enzyme (*27*). In order to identify regions in the prodomain involved in the inhibition of the catalytic domain, we started by asking how selective TACE is for interactions with ADAM prodomains. We chose candidate ADAM prodomains for these studies based on examination of primary sequence alignments of the entire family and selected two that represented phylogenetic extremes relative to TACE, ADAM 9, and ADAM 10. Despite extremely poor sequence homology among ADAM prodomains, 23% of ADAM 10 residues were identical to TACE within this region; in contrast, only 14% of ADAM 9 residues were identical to TACE (Figure 1).

Next, we tested whether the prodomains of ADAM 9 and ADAM 10 were capable of inhibiting the proteolytic activity of the catalytic domain of TACE. For that, we expressed and purified the prodomains of ADAM 9, ADAM 10, and TACE. Surprisingly, even though the prodomain region of ADAM 10 displays only 23% sequence identity relative to its TACE counterpart (Figure 1), isolated ADAM 10 prodomain was as potent in inhibiting TACE as the cognate prodomain of this enzyme (IC_{50} = 75 nM; Figure 2); in contrast, the prodomain of ADAM 9, showing lesser sequence conservation (14% identity), was a poor inhibitor of TACE (IC_{50} > 4 μM; Figure 2). This means that even though the prodomain of ADAM 10 shows an overall low level of sequence identity to TACE, key residues accounting for its inhibitory function not present in the ADAM 9 prodomain must have been conserved.

Identification of TACE Prodomain Regions Critical for Inhibition of the TACE Catalytic Domain. Further analysis of the amino acid sequences of the prodomain of TACE versus ADAM family members revealed two short regions that were dramatically different in TACE and ADAM10 relative to all other ADAM prodomains (Figure 3): region 1 (TACE residues 72−96) showed a relatively high degree of conservation only between TACE and ADAM10 (50% identity), with no significant homology to other family members; region 2 (TACE residues 114−137) displayed a strikingly high level of identity (~67%) for virtually all ADAMs, except for TACE and ADAM 10. Therefore, this higher resolution analysis of ADAM sequences indicated that TACE and ADAM 10 prodomains appear to have evolved unique determinants for their interaction with their respective catalytic domains. We hypothesize that these two regions may account for the functional equivalency of TACE and ADAM 10 isolated prodomains for enzyme inhibition.

To test this hypothesis, we asked whether regions 1 and 2 determined the differential properties of ADAM 9 and ADAM 10 prodomains as TACE inhibitors. We prepared constructs of the TACE prodomain encoding the corresponding ADAM 9 residues at region 1 or 2, as well as constructs containing permutations in only the left or right half-segments of each of those two regions, as shown in Figure 4. All chimeric polypeptides showed expression, purification, and solution properties comparable to wild-type TACE prodomain (*27*). The ADAM 9 region 1-substituted TACE prodomain as well as the left half (region 1A) substituted variant entirely lost inhibitory potency against TACE catalytic domain (Figure 5A). In contrast, the chimera containing the right half of ADAM 9 region 1 (region 1B) was as potent at inhibiting TACE as the wild-type TACE prodomain (Figure 5A). Thus, TACE prodomain motif FSALKRHFKL81 is essential for inhibition of the catalytic domain function. ADAM 9 region 2 chimeras also affected the inhibitory function of TACE prodomain. Variants containing an entire

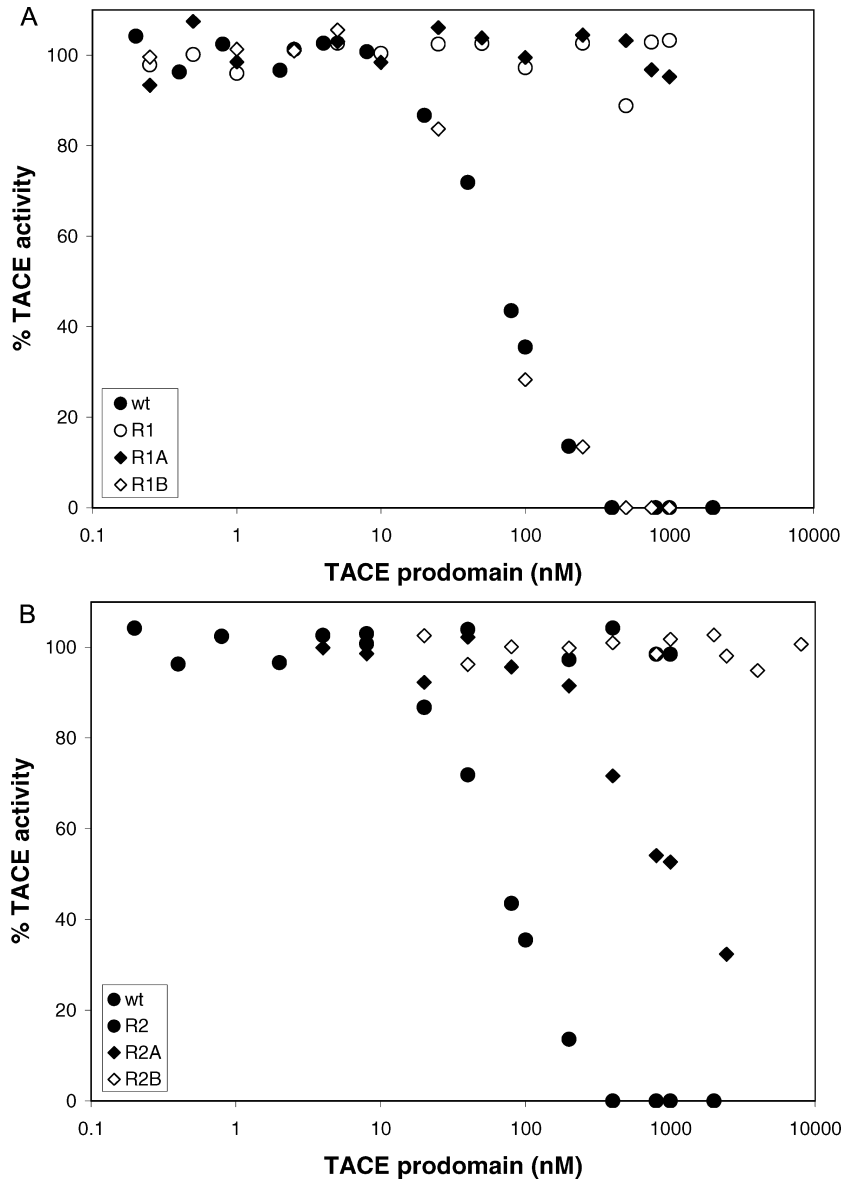

FIGURE 5: Inhibition of TACE catalytic domain (residues 215−473) by recombinant, purified TACE/ADAM 9 prodomain region 1 (panel A) or region 2 (panel B) chimeras described in Figure 4. Wild-type prodomain inhibition values are shown for comparison. Each curve is representative of at least three experiments.

ADAM 9 region 2 substitution as well as the ones containing the left (region 2A) or right (region 2B) half of that ADAM 9 region were either inactive or inhibited TACE only partially ($IC_{50} > 2\ \mu M$ for region 2A; region 2 and region 2B entirely lost inhibitory potency; Figure 5B).

We next focused on TACE prodomain regions 1A and 2B, as they exhibited the most dramatic phenotypes in terms of inhibitory function over the activity of TACE catalytic domain. We constructed two single site mutants, F72V within region 1A and a substitution in region 2B where the ADAM consensus sequence GLRG was replaced for the TACE sequence DDVI at residues 134−137 (GLRG137). As shown in Figure 6, both of those variants exhibited decreases in inhibitory potency relative to wild-type TACE prodomain ($IC_{50} > 0.6\ \mu M$ for F72V and $>3\ \mu M$ for GLRG137). In comparison to ADAM 9 prodomain inhibitory potency, the region 1 point variant F72V appeared to be more potent, while the GLRG137 variant appeared to have a similar inhibitory effect.

TACE/ADAM 9 Prodomain Chimeras Are Stably Folded Polypeptides. The chimeric proteins that we have engineered depart significantly from the sequence of the wild-type TACE prodomain. Therefore, it could be argued that the observed losses in inhibitory function are the result of dramatic alterations in the folding properties of these variant prodomains. In order to address this possibility, we examined the secondary structure of all inactive TACE/ADAM 9 prodomains by circular dichroism spectroscopy. We have shown before that the TACE prodomain folds stably in isolation, showing circular dichroism spectra consistent with predominant helix-loop secondary structure content (*27*). Relative to the wild-type TACE prodomain, all inactive variants showed similar secondary structure content, suggesting that their overall fold and stability at room temperature are not substantially different. As an illustration, the circular dichroism profiles of the entire region 1 and region 2 mutants, and wild-type TACE prodomain, are shown in Figure 7.

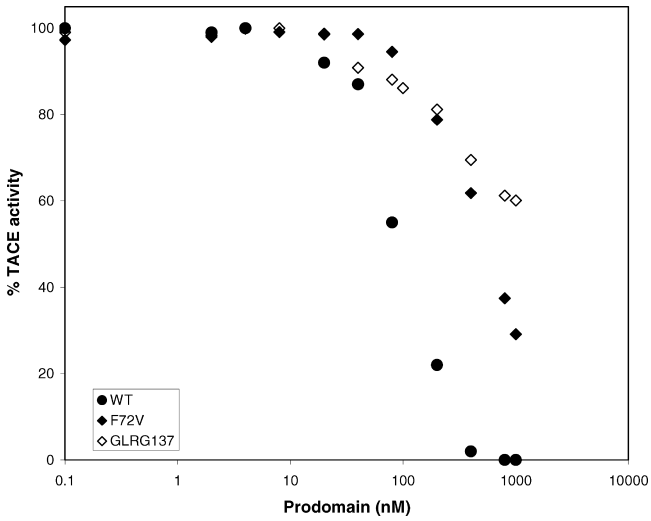

FIGURE 6: Inhibition of TACE catalytic domain (residues 215−473) by recombinant, purified TACE prodomain site-directed variants F72V and GLRG137. Wild-type prodomain inhibition values are shown for comparison. Each curve is representative of at least three experiments.

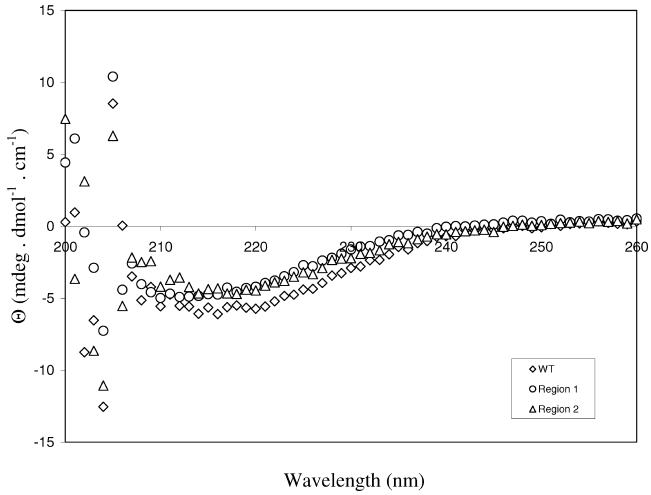

FIGURE 7: Secondary structure content of recombinant, isolated wild-type TACE prodomain and fully inactive TACE/ADAM 9 prodomain chimeras region 1, region 1A, region 2, and region 2B.

DISCUSSION

The prodomains of ADAMs are relatively large when compared to the ones of most metalloproteases biosynthesized in precursor, inactive forms. An available structural model of the matrix metalloproteinase-2 zymogen reveals that its prodomain serves fundamentally a local role, occluding the active site (*37*). Enzyme activation usually occurs in an autocatalytic fashion, probably related to the ability of the active site to disengage and cleave its prodomain at one or more places (*38, 39*). In contrast, for many ADAM zymogens proprotein converting enzymes of the furin/Kex-2 family mediate that maturation event (*32, 33*). ADAM 8 seems to behave in an exceptional manner: its zymogen appears to convert to the mature form in an autocatalytic fashion (*19*). It may be possible that our previous observations with the TACE zymogen extend to other ADAM family members and the zymogen state is actually a prodomain−catalytic domain complex in which the latter domain is arrested in its folding. Should that be the case, the interacting sites between these two domains may be extensive and diffusely located. This may explain the relatively large size of ADAM prodomains.

The prodomain of TACE consists of 214 amino acid residues minus the signal peptide (18 residues). In the absence of a structural model or any information on constraints, the development of computational models to predict the three-dimensional of this domain and its mode of interaction with the catalytic domain is not feasible. Therefore, only the combination of genetic and biochemical approaches may yield at this point any data to map contact sites across both domains. We know from N-terminal sequencing analysis that the secreted prodomain of TACE (as part of the prodomain−catalytic domain complex) starts at residue Asp59 (*17*). Additionally, our mutational analysis of the C-terminal cysteine switch and vicinal residues indicated that positions downstream from residue Gln179 are not important for the inhibitory activity of the prodomain or its chaperone function, either (*27*). These two pieces of information, when taken together, suggest that a minimal TACE prodomain retaining all information for interaction with the catalytic domain spans positions Asp59 to Gln179, or 121 residues. Finding key determinants for both the chaperone and inhibitory functions within that sequence space is still a challenging task.

Phylogenetic analysis is a proven strategy for identifying functionally critical residues in the otherwise vast sequence space of most proteins. We decided to follow that approach to the identification of TACE prodomain residues determining its inhibitory function. Unexpectedly, we readily identified two discontinuous regions in TACE and ADAM 10 showing evolutionary uniqueness relative to other ADAMs, regions 1 and 2 (Figure 3), suggesting that the catalytic domain binding epitopes on TACE prodomain must be discontinuous. In fact, our results show that variants of the prodomain of TACE containing permutations to ADAM 9 residues either in region 1 or in region 2 resulted in a loss of inhibitory potency. This observation is not surprising: It has been shown for several protein−protein interfaces that critical residues are not necessarily contiguous on the polypeptide chain primary sequence (*40*−*43*). On the other hand, certain prodomain positions show conservation across all ADAM family members examined (Figure 1). Why? It may be possible that at least some of those residues have important roles in determining the general architecture (folding) or thermodynamic stability of this domain of the enzyme.

From further mutational analysis of regions 1 and 2, we reach the conclusion that TACE prodomain segments 1A (FSALKRHFKLY82) and 2B (RVLAHIRDDDVI137) contain residues of critical importance for its inhibitory function: substitutions at these subregions fully eliminate the ability of those prodomain variants to inhibit TACE. We have done a preliminary assessment of key residues within these subregions. Residue Phe72 is identical in TACE and ADAM 10, yet other ADAM prodomains contain a much smaller hydrophobic residue at that position (Val, Leu, Ile; Figure 3). We found that TACE prodomain variant F72V was nearly 10-fold less potent as an inhibitor of TACE relative to the wild-type prodomain ($IC_{50} > 0.6$ μM, Figure 6). The triplet RHF79, also within subregion 1A, is also identical between TACE and ADAM only. We do not know yet how mutation of that triplet in TACE prodomain affects its inhibitory

function. Because F72V exhibited higher potency that the ADAM 9 prodomain, we hypothesize that the triplet RHF79 must also determine the interaction of TACE with its prodomain. With regard to region 2, the most remarkable difference between TACE prodomain subregion 2B and other ADAMs is the presence of the sequence DDVI137 where virtually all other ADAMs display the highly conserved motif GLRG. Not surprisingly, introduction of the GLRG consensus motif at TACE positions 134−137 decreased the inhibitory function almost to the same level observed with ADAM 9 prodomain ($IC_{50} > 3$ μM). Therefore, we can tentatively establish at this point residues Phe72 and the motif Asp-Asp-Val-Ile137 as critical epitopes for TACE prodomain association and inhibition of the catalytic domain. By inference, the motif Arg-His-Phe79 may play a role that remains to be evaluated.

Region 1 and 2 variants described here contain multiple single point substitutions that may have nonlocal effects on the conformation and structural stability of the polypeptide. Therefore, as in any structure−function study, ultimate proof that the mutation has an effect solely on aspects of the contact interface with TACE catalytic domain can only be obtained via structural analysis. Regretfully, there is at this point no crystallographic or NMR means allowing us to perform such assessment. Because the prodomain of TACE folds in a highly cooperative manner, its spectroscopic signature for secondary structure (measured by circular dichroism) is a useful tool for low-resolution assessment of correct folding and near-wild-type structural stability. This readout is particularly sensitive for the TACE prodomain because is only marginally stable at room temperature (*27*). Therefore, the secondary structure content measured via circular dichroism provides a way of comparing the thermodynamic stability of its variants relative to wild type. As shown in Figure 7, even variants exhibiting a total loss of activity were essentially indistinguishable from wild-type TACE prodomain in their secondary structure content (molar ellipticity in the far-ultraviolet range). As an independent way to evaluate the function of those mutants, we attempted to measure their activity as inhibitors of ADAM 9, the enzyme counterpart used for the design of TACE prodomain variants. Although we were able to obtain ADAM 9 catalytic domain in isolation, available substrates were processed very inefficiently, preventing accurate quantification (*44*).

We know from earlier studies that the dissociation constant for the prodomain−catalytic domain complex falls within the nanomolar range ($IC_{50} = 75$ nM), and we have shown that synthetic peptides comprising the cysteine switch can only account for affinity in the low micromolar range (*27*). As our data show, other residues in the prodomain contribute significantly to the stability of the complex. A careful study recently published by Moss and co-workers shows that this also applies to ADAM 10 inhibition by its prodomain (*20*). This report also shows that the TACE prodomain can also inhibit ADAM 10 and ADAM 8, although less potently. A surprising finding in that study is that the prodomain of ADAM 10 seems to be equally potent against forms of that enzyme comprising the catalytic domain only and the catalytic plus disintegrin/cysteine-rich domain. For TACE, the prodomain is a poor inhibitor of the longer form ($IC_{50} > 3$ μM; *27*). This is the reason why we have done these studies with the TACE catalytic domain form: the prodomain inhibits it potently enough to allow accurate measurement of functional effects of mutations.

It is important to point out that the region 2 sequence is actually very different in TACE vs ADAM 10 prodomain. Therefore, while there is functional equivalence for these two domains, the geometry of interaction with their respective catalytic domains may be different. The crystallographic structure of the catalytic domain of TACE shows that this enzyme contains large loops that are not present in previously solved matrix metalloproteinase structures (*45*). Structures of the catalytic domain of ADAM 10, the mature extracellular domains (catalytic plus disintegrin/cysteine-rich) of TACE and ADAM 10, or their zymogen forms have not been solved yet. It remains possible that the positioning of the disintegrin/cysteine-rich domain relative to the catalytic and prodomains may create steric hindrance for TACE but not for ADAM 10. Clearly, a three-dimensional structure of prodomain−catalytic complexes for these two ADAMs will be very useful in addressing the nature of these differences. At this point, cocrystallization of the prodomain−catalytic domain complex of ADAM 10 seems promising, because the prodomain of ADAM 10 shows expression, purification, and solution properties more amenable with crystallization activities, relative to TACE (*20, 27*). The crystallographic structure of the prodomain−catalytic domain complex for TACE or ADAM 10 will be useful for the identification of additional residues to mutagenize and test functionally. By following this approach in a systematic way, a functional map can be constructed to annotate the crystallographic structure of the prodomain−catalytic domain interface. That information is critical to validate the "arrested folding" model that we have proposed to account for ADAM prodomain mechanism of inhibition of their cognate catalytic domains (*18, 46, 47*).

ACKNOWLEDGMENT

We thank Soo-Hwa Kim, Mohita Mohan, Frank Lin, and Amol Pawar for help and discussions. We also thank Professor Walter Englander for spectropolarimeter access.

REFERENCES

1. Black, R. A., Rauch, C. T., Kozlosky, C. J., Peschon, J. J., Slack, J. L., Wolfson, M. F., Castner, B. J., Stocking, K. L., Reddy, P., Srinivasan, S., Nelson, N., Boiani, N., Schooley, K. A., Gerhart, M., Davis, R., Fitzner, J. N., Johnson, R. S., Paxton, R. J., March, C. J., and Cerretti, D. P. (1997) A metalloproteinase disintegrin that releases tumour necrosis factor-α from cells. *Nature 385*, 729–733.
2. Moss, M. L., Jin, C., Milla, M. E., Bickett, D. M., Buckhart, W., Carter, H. L., Chen, W.-J., Clay, W. C., Didsbury, J., Hassler, D., Kost, T. A., Lambert, M. H., Leesnitzer, M. A., McCauley, P., McGeehan, G., Moyer, M., Pahel, G. L., Rocque, W., Seaton, T., Su, J.-L., Warner, J., Willard, D., and Becherer, D. (1997) Cloning of a disintegrin metalloproteinase that processes precursor tumor-necrosis factor-α. *Nature 385*, 733–736.
3. Peschon, J. J., Slack, J. L., Reddy, P., Stocking, K. L., Sunnaborg, S. W., Lee, D. C., Russell, W. E., Castner, B. J., Johnson, R. S., Fitzner, J. N., Boyce, R. W., Nelson, N., Kozlosky, C. J., Wolfson, M. F., Rauch, C. T., Cerretti, D. P., Paxton, R. J., March, C. J., and Black, R. A. (1998) An essential role for ectodomain shedding in mammalian development. *Science 282*, 1279–1280.
4. Sunnarborg, S. W., Hinkle, C. L., Stevenson, M., Russell, W. E., Raska, C. S., Peschon, J. J., Castner, B. J., Gerhart, M. J., Paxton, R. J., Black, R. A., and Lee, D. C. (2002) Tumor necrosis factor-alpha converting enzyme (TACE) regulates epidermal growth factor receptor ligand availability. *J. Biol. Chem. 277*, 12838–12845.
5. Mohan, M. J., Seaton, T., Hassler, D., Blackburn, R. K., Burkhart, W., Moyer, M., Mitchell, J., Waitt, S., Becherer, J. D., Moss, M. L.,

and Milla, M. E. (2002) Substrate requirements of the tumor necrosis factor-alpha converting enzyme (TACE). *Biochemistry 41*, 9462–9469.
6. Hinkle, C. L., Mohan, M. J., Lin, P., Yeung, N., Rasmussen, F., Milla, M. E., and Moss, M. L. (2003) Multiple metalloproteinases process protransforming growth factor-alpha (proTGF-alpha). *Biochemistry 42*, 2127–2136.
7. Wang, J., Al-Lamki, R. S., Zhang, H., Kirkiles-Smith, N., Gaeta, M. L., Thiru, S., Pober, J. S., and Bradley, J. R. (2003) Histamine antagonizes TNF signaling by stimulating TNF receptor shedding from the cell surface and golgi storage pool. *J. Biol. Chem. 278*, 21751–21760.
8. Jackson, L. F., Qiu, T. H., Sunnarborg, S. W., Chang, A., Zhang, C., Patterson, C., and Lee, D. C. (2003) Defective valvulogenesis in HB-EGF and TACE-null mice is associated with aberrant BMP signaling. *EMBO J. 22*, 2704–2716.
9. Rio, C., Buxbaum, J. D., Peschon, J. J., and Corfas, G. (2000) Tumor necrosis factor-alpha-converting enzyme is required for cleavage of erbB4/HER4. *J. Biol. Chem. 275*, 10379–10387.
10. Zhang, Y., Jiang, J., Black, R. A., Baumann, G., and Frank, S. J. (2000) Tumor necrosis factor-alpha converting enzyme (TACE) is a growth hormone binding protein (GHBP) sheddase: the metalloprotease TACE/ADAM-17 is critical for (PMA-induced) GH receptor proteolysis and GHBP generation. *Endocrinology 141*, 4342–4348.
11. Rovida, E., Paccagnini, A., Del Rosso, M., Peschon, J., and Dello Sbarba, P. (2001) TNF alpha converting enzyme cleaves the macrophage colony-stimulating factor receptor in macrophages undergoing activation. *J. Immunol. 166*, 1583–1589.
12. Brou, C., Logeat, F., Gupta, N., Bessia, C., LeBail, O., Doedens, J. R., Cumano, A., Roux, P., Black, R. A., and Israel, A. (2000) A novel proteolytic cleavage involved in Notch signaling: the role of the disintegrin-metalloprotease TACE. *Mol. Cell 5*, 207–216.
13. Buxbaum, J. D., Liu, K. N., Luo, Y., Slack, J. L., Stocking, K. L., Peshon, J. J., Johnson, R. S., Castner, B. J., Cerretti, D. P., and Black, R. A. (1998) Evidence that tumor necrosis factor alpha converting enzyme is involved in regulated alpha-secretase cleavage of the Alzheimer amyloid protein precursor. *J. Biol. Chem. 273*, 27765–27767.
14. Skovronsky, D. M., Moore, D. B., Milla, M. E., Doms, R. W., and Lee, V. M.-Y. (2000) PKC-dependent α-secretase competes with β-secretase for cleavage of APP in the TGN. *J. Biol. Chem. 275*, 2568–2575.
15. Skovronsky, D. M., Fath, S., Lee, V. M.-Y., and Milla, M. E. (2001) Neuronal localization of the TNFα converting enzyme (TACE) in brain tissue and its relationship to amyloidogenesis. *J. Neurobiol. 49*, 40–46.
16. Vincent, B., Paitel, E., Saftig, P., Frobert, Y., Hartmann, D., De Strooper, B., Grassi, J., Lopez-Perez, E., and Checler, F. (2001) The disintegrins ADAM10 and TACE contribute to the constitutive and phorbol ester-regulated normal cleavage of the cellular prion protein. *J. Biol. Chem. 276*, 37743–37746.
17. Milla, M. E., Leesnitzer, M. A., Moss, M. L., Clay, W. C., Carter, H. L., Miller, A. B., Su, J.-L., Lambert, M. H., Willard, D. H., Sheeley, D. M., Kost, T. A., Burkhart, W., Moyer, M., Blackburn, R. K., Pahel, G. L., Mitchell, J. L., Hoffman, C. R., and Becherer, J. D. (1999) Specific sequence determinants are required for the expression of functional tumor necrosis factor-α converting enzyme (TACE). *J. Biol. Chem. 274*, 30563–30570.
18. Leonard, J. D., Lin, F., and Milla, M. E. (2004) Chaperone-like properties of the pro-domain of TACE and the role of its cysteine switch. *Biochem. J. 387*, 797–805.
19. Moss, M. L., Bomar, M., Liu, Q., Sage, H., Dempsey, P., Lenhart, P. M., Gillispie, P. A., Stoeck, A., Wildeboer, D., Bartsch, J. W., Palmisano, R., and Zhou, P. (2007) The ADAM10 prodomain is a specific inhibitor of ADAM10 proteolytic activity and inhibits cellular shedding events. *J. Biol. Chem. 282*, 35712–35721.
20. Schlomann, U., Wildeboer, D., Webster, A., Antropova, O., Zeuschner, D., Knight, C. G., Docherty, A. J., Lambert, M., Skelton, L., Jockusch, H., and Bartsch, J. W. (2002) The metalloprotease disintegrin ADAM8. Processing by autocatalysis is required for proteolytic activity and cell adhesion. *J. Biol. Chem. 277*, 48210–48219.
21. Roghani, M., Becherer, J. D., Moss, M. L., Atherton, R. E., Erdjument-Bromage, H., Arribas, J., Blackburn, R. K., Weskamp, G., Tempst, P., and Blobel, C. (1999) Metalloprotease-disintegrin MDC9: intracellular maturation and catalytic activity. *J. Biol. Chem. 274*, 3531–3540.
22. Anders, A., Gilbert, S., Garten, W., Postina, R., and Fahrenholz, F. (2001) Regulation of the alpha-secretase ADAM10 by its prodomain and proprotein convertases. *FASEB J. 15*, 1837–1839.
23. Loechel, F., Overgaard, M. T., Oxvig, C., Albrechtsen, R., and Wewer, U. M. (1999) Regulation of human ADAM 12 protease by the prodomain. Evidence for a functional cysteine switch. *J. Biol. Chem. 274*, 13427–13433.
24. Sundberg, C., Thodeti, C. K., Kveiborg, M., Larsson, C., Parker, P., Albrechtsen, R., and Wewer, U. M. (2004) Regulation of ADAM12 cell-surface expression by PKC epsilon. *J. Biol. Chem. 279*, 51601–51611.
25. Lum, L., Reid, M. S., and Blobel, C. P. (1998) Intracellular maturation of the mouse metalloprotease disintegrin MDC15. *J. Biol. Chem. 273*, 26236–26247.
26. Schlöndorff, J., Becherer, J. D., and Blobel, C. P. (2000) Intracellular maturation and localization of the tumour necrosis factor alpha convertase (TACE). *Biochem. J. 347*, 131–138.
27. Gonzales, P. E., Solomon, A., Miller, A. B., Leesnitzer, M. A., Sagi, I., and Milla, M. E. (2004) Inhibition of the tumor necrosis factor-α-converting enzyme by its pro domain. *J. Biol. Chem. 279*, 31638–31645.
28. Kang, T., Zhao, Y. G., Pei, D., Sucic, J. F., and Sang, Q. X. (2002) Intracellular activation of human adamalysin 19/disintegrin and metalloproteinase 19 by furin occurs via one of the two consecutive recognition sites. *J. Biol. Chem. 277*, 25583–25591.
29. Howard, L., Maciewicz, R. A., and Blobel, C. P. (2000) Cloning and characterization of ADAM28: evidence for autocatalytic pro-domain removal and for cell surface localization of mature ADAM28. *Biochem. J. 348*, 21–27.
30. Galazka, G., Windsor, L. J., Birkedal-Hansen, H., and Engler, J. A. (1996) APMA (4-aminophenylmercuric acetate) activation of stromelysin-1 involves protein interactions in addition to those with cysteine-75 in the propeptide. *Biochemistry 35*, 11221–11227.
31. van Wart, H., and Birkedal-Hansen, B. (1990) The cysteine switch: a principle of regulation of metalloprotease activity with potential applicability to the entire matrix metalloprotease gene family. *Proc. Natl. Acad. Sci. U.S.A. 87*, 5578–5581.
32. Endres, K., Anders, A., Kojro, E., Gilbert, S., Fahrenholz, F., and Postina, R. (2003) Tumor necrosis factor-alpha converting enzyme is processed by proprotein-convertases to its mature form which is degraded upon phorbol ester stimulation. *Eur. J. Biochem. 270*, 2386–2393.
33. Srour, N., Lebel, A., McMahon, S., Fournier, I., Fugère, M., Day, R., and Dubois, C. M. (2003) TACE/ADAM-17 maturation and activation of sheddase activity require proprotein convertase activity. *FEBS Lett. 554*, 275–283.
34. Chantry, A., Gregson, N. A., and Glynn, P. (1989) A novel metalloproteinase associated with brain myelin membranes. Isolation and characterization. *J. Biol. Chem. 264*, 21603–21607.
35. Lammich, S., Kojro, E., Postina, R., Gilbert, S., Pfeiffer, R., Jasionowski, M., Haass, C., and Fahrenholz, F. (1999) Constitutive and regulated alpha-secretase cleavage of Alzheimer's amyloid precursor protein by a disintegrin metalloprotease. *Proc. Natl. Acad. Sci. U.S.A. 96*, 3922–3927.
36. Howard, L., Lu, X., Mitchell, S., Griffiths, S., and Glynn, P. (1996) Molecular cloning of MADM: a catalytically active mammalian disintegrin-metalloprotease expressed in various cell types. *Biochem. J. 317*, 45–50.
37. Morgunova, E., Tuuttila, A., Bergmann, U., Isupov, M., Lindqvist, Y., Schneider, G., and Tryggvason, K. (1999) Structure of human pro-matrix metalloproteinase-2: activation mechanism revealed. *Science 284*, 1667–1670.
38. Imai, K., Yokohama, Y., Nakanishi, I., Ohuchi, E., Fujii, Y., Nakai, N., and Okada, Y. (1995) Matrix metalloproteinase 7 (matrilysin) from human rectal carcinoma cells. Activation of the precursor, interaction with other matrix metalloproteinases and enzymic properties. *J. Biol. Chem. 270*, 6691–6697.
39. Nagase, H., Suzuki, K., Morodomi, T., Enghild, J. J., and Salvesen, G. (1992) Activation mechanisms of the precursors of matrix metalloproteinases 1, 2 and 3. *Matrix Suppl. 1*, 237–244.
40. Clackson, T., and Wells, J. A. (1995) A hot spot of binding energy in a hormone-receptor interface. *Science 267*, 383–386.
41. Wrighton, N. C., Farrell, F. X., Chang, R., Kashyap, A. K., Barbone, F. P., Mulcahy, L. S., Johnson, D. L., Barrett, R. W., Jolliffe, L. K., and Dower, W. J. (1996) Small peptides as potent mimetics of the protein hormone erythropoietin. *Science 273*, 458–464.

42. Wiesmann, C., and de Vos, A. M. (2000) Variations on ligand-receptor complexes. *Nat. Struct. Biol. 7*, 440–442.
43. Clackson, T., Ultsch, M. H., Wells, J. A., and de Vos, A. M. (1998) Structural and functional analysis of the 1:1 growth hormone: receptor complex reveals the molecular basis for receptor affinity. *J. Mol. Biol. 277*, 1111–1128.
44. Gonzales, P. E. (2005) Inhibition of the tumor necrosis factor-α converting enzyme by its prodomain, Ph.D. Dissertation, University of Pennsylvania, Philadelphia, PA (UMI number 3165683, Section 4.3.2.3.1, p 92).
45. Maskos, K., Fernandez-Catalan, C., Huber, R., Bourenkov, G. P., Bartunik, H., Ellestad, G. A., Reddy, P., Wolfson, M. F., Rauch, C. T., Castner, B. J., Davis, R., Clarke, H. R. G., Petersen, M., Fitzner, J. M., Cerretti, D. P., March, C. J., Paxton, R. J., Black, R. A., and Bode, W. (1998) Crystal structure of the catalytic domain of human tumor necrosis factor-α converting enzyme. *Proc. Natl. Acad. Sci. U.S.A. 95*, 3408–3412.
46. Sagi, I., and Milla, M. E. (2007) Novel dynamic approaches provide insights into the enzymatic mechanism of matrix metalloproteinases. *Anal. Biochem. 372*, 1–10.
47. Milla, M. E., Gonzales, P. E., and Leonard, J. D. (2006) The TACE zymogen: re-examining the role of the cysteine-switch. *Cell Biochem. Biophys. 44*, 342–348.

BI801049V